Ligand–metal interactions and excited state properties in ruthenium(II)–diimine complexes

Talal S. Akasheh*, Ibrahim Jibril and **Amjad M. Shraim**
Chemistry Department, Yarmouk University, Irbid (Jordan)

(Received November 21, 1989)

Abstract

2,2′-Bipyridine (bpy); 2,2′-bipyrazine (bpz); 5,6-dimethyl-2,3-di-(2′-pyridyl)-quinoxaline (dbpq); 4,4′-dimethyl-2,2′-bipyridine (dmbpy), 2,3-di-(2′-pyridyl)-pyrazine (dpp); 3,3′-bipyridazine (bpd); 2,3-di-(2′-pyridyl)-quinoxaline (dpq) and 2-(2′-pyridyl)-quinoline (pyq) form mixed-ligand complexes with Ru(II). The excited state properties (emission, lifetimes and redox potentials) are reported and analyzed in the framework of solar energy conversion. Ligand σ- and π-bonding properties are also deduced.

Introduction

The search for good solar energy converters among various ruthenium(II) diimine complexes focuses on the properties of the luminescent ^{3}MLCT state (triplet metal to ligand charge transfer state) which is responsible for photosensitization of the various electron transfer quenching processes that lead to the photogalvanic effect [1–5] and/or the reduction of water to hydrogen [1–11]. A highly efficient intersystem crossing from the lowest singlet (^{1}MLCT) [12–14] and a relatively long triplet state lifetime render the quenching processes more competitive. On the other hand, the thermal population of a closely lying d–d state from the ^{3}MLCT state leads to photochemical substitution [15–28] which interferes with energy conversion. Obviously the redox properties of the ^{3}MLCT play an important role in determining the success of a particular complex in efficient energy conversion.

The above mentioned properties are very sensitive to the choice of ligands coordinated to the metal atom. Typically, the use of substituents [29] on a particular ligand has been used to raise the d–d state out of reach of thermal population. Variation of the ligands themselves have also been studied [13, 30, 31]. Cyclic voltammetry presents itself as a very attractive probe of the effect of various ligands. For one thing, ground state redox potentials in combination with emission results may be used to estimate the excited state redox potentials [30–33]. This is a result of the fact that orbitals involved in the ground state electrochemical process and the optical excitation are the same (namely the lowest unoccupied orbital (LUMO) of the ligand and the highest occupied metal orbital (HOMO) of t_{2g} origin in octahedral symmetry). Furthermore, the oxidation potential and the first reduction potential give an idea about the relative stabilities of the metal HOMO d-orbital and the ligand LUMO orbital, respectively. These stabilities can consequently be interpreted to compare the σ-donor and the π-acceptor ability of the ligand [30–32, 34–37]. While it may be difficult to exactly assess how these metal–ligand interactions directly affect the behaviour of the ^{3}MLCT state, there could be no doubt that they play an important role in providing the right conditions for efficient photosensitization.

In pursuit of new photosensitizers, we have recently prepared the tris complex $[Ru(dbpq)_3]^{2+}$ as well as a number of complexes of the mixed ligand type $RuL_2L'^{2+}$ as the PF_6 salts with L = bpy, bpz, dbpq, dmbpy, dpp; L′ = bpd, dbpq, bpq, bpy (not all combi-

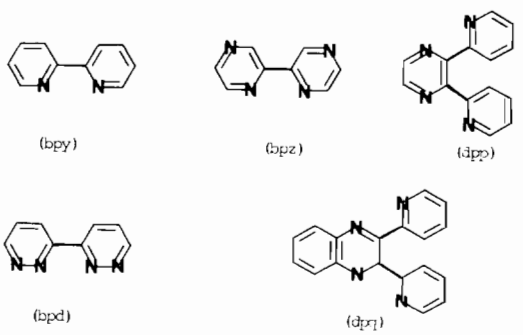

*Author to whom correspondence should be addressed.

0020-1693/90/$3.50

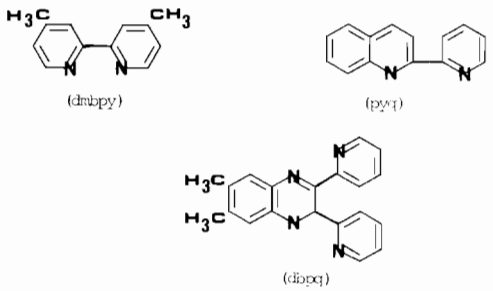

nations of L and L′ are covered – see results). The excited state characteristics of the complexes and the σ- and π-properties of the ligands are reported in this paper. In order to obtain a more complete picture, the results for various tris and mixed-ligand complexes reported in the literature are also analyzed.

Experimental

All complexes in this study have been prepared by standard procedures and will be reported elsewhere [38]. Solvents used for physical measurements were of HPLC type. Luminescence and UV–Vis spectra were recorded on a Perkin-Elmer MPF-44B fluorescence spectrophotometer and Varian 2300 series spectrophotometer, respectively. Lifetimes were measured on a K-347 Applied Photophysics laser flash photolysis system in emission mode along with a Spectron Nd:YAG laser (6–9 ns). Cyclic voltammetry was recorded using a Hi-Tech Potentiostat in DMF for reductions and acetonitrile for oxidations. The supporting electrolyte was tetra-n-butylammonium hexafluorophosphate (0.1 M). The sweep speed was 0.1 V/s, while the working and counter electrodes were Pt. For reference, the SSCE electrode was used.

Results and discussion

UV–Vis spectra

Table 1 shows the UV–Vis results. In general the region above 400 nm shows broad intense MLCT ($d\pi$–π^*) bands. The sharp highly intense UV peaks are usually ligand centered π,π^* transitions that are also observed in the free ligand. This region may also contain ligand n,π^* transitions that are usually weak and difficult to discern (often appearing as shoulders). In the region 300–400 nm, a number of peaks that are of comparable or slightly higher intensity than the MLCT bands are often assigned as MLCT bands to higher ligand π^* states [31]. However, the possibility of LMCT (ligand to metal charge transfer) and/or d–d (metal centered) transitions cannot be entirely ruled out. While the above comments are a bit general, more specific assignments can be made upon examination of the spectra. This, however, is made difficult by the overlap of the broad peaks in the mixed-ligand complexes.

In Fig. 1 the UV–Vis spectra of $[Ru(dbpq)_3]^{2+}$, $[Ru(bpy)(dbpq)_2]^{2+}$ and $[Ru(bpy)_2(dbpq)]^{2+}$ are shown. The general comments regarding the MLCT and π,π^* features apply very well to the three complexes. At first glance, substitution of bpy for dbpq in $[Ru(dbpq)_3]^{2+}$ appears to induce new peaks that are related to bpy. By comparison to $[Ru(bpy)_3]^{2+}$ (451, 345, 323, 285, 250, 238 nm [31]) it is clear that the peaks at 352, 285 and 254 could be related to bpy. A closer examination of the extinction coefficients (a plot of ϵ versus λ, not shown here, illustrates this point very well) shows that the major features in $[Ru(dbpq)_3]^{2+}$ are drastically reduced in intensity when stepwise replacement of dbpq occurs. Based on this fact, it becomes clear that the main π,π^* peak around 258 nm and the broad features at 388 and 331 (or 352) as well as the lowest energy MLCT bands are dominated by dbpq in $[Ru(bpy)_2dbpq]^{2+}$ and $[Ru(bpy)(dbpq)_2]^{2+}$. A shoulder at 274 nm in the former complex, a peak and a shoulder (at 255) in both complexes, respectively and a peak at 460 nm in the second complex, but blue shifted to 430 in the first, are all assignable to bpy related transitions. The low energy 469 nm MLCT band in $[Ru(dbpq)_3]^{2+}$ ($d\pi$–π^* of dbpq) is red shifted in the mixed-ligand complexes as is commonly observed [30, 31]. The red shift is due to the better σ-donation of bpy which destabilizes the metal orbital. This aspect will be discussed more fully in a later section. The fact that $[Ru(dbpq)_2(bpy)]^{2+}$ exhibits a larger red shift than $[Ru(dbpq)(bpy)_2]^{2+}$ is surprising. However, the broadness of the peaks, complicated by the fact that the weak ^{3}MLCT absorption might be responsible for the long tail in the ^{1}MLCT lowest energy peak [30, 31] could render the exact determination of the shift very difficult. In contrast, a blue shift occurs in $[Ru(bpz)_2dbpq]^{2+}$ with the lowest energy dbpq MLCT band appearing at 450 nm. This is clearly shown in Fig. 2, which also includes the UV–Vis spectra of $[Ru(bpz)_2bpd]^{2+}$ and $[Ru(bpy)_2bpd]^{2+}$. The 230 nm peak in $[Ru(bpz)_2dbpq]^{2+}$ is reminiscent of $[Ru(bpz)_3]^{2+}$ at 240 nm [31]. Other peaks are more difficult to assign but the 355 nm shoulder could be due to bpz and/or dbpq, while the 395 nm shoulder is more likely to be due to dbpq (383 nm broad shoulder in $[Ru(dbpq)_3]^{2+}$). Fortunately, the situation is much more clearcut in $[Ru(bpz)_2(bpd)]^{2+}$, since the results for $[Ru(bpz)_3]^{2+}$ (440, 338 (sh), 291 and 240 nm [40]) and for $[Ru(bpd)_3]^{2+}$ in water (449, 444, 410, 363, 265 and 234 nm [32]) indicate

TABLE 1. UV–Vis spectral data in acetonitrile[a]

Compound	λ (nm) ($\epsilon \times 10^{-4}$ (dm^3 mol^{-1} cm^{-1}))			
$[Ru(bpy)_2(bpd)]^{2+}$	472(1.33) 258(sh)	410(1.56) 241(3.02)	360(sh) 206(6.82)	278(6.61)
$[Ru(bpy)_2(dbpq)]^{2+}$	510(0.91) 285(9.38)	430(0.94) 274(sh)	383(sh) 254(1.53)	352(sh)
$[Ru(bpz)_2(bpd)]^{2+}$	446(2.44) 276(sh)	414(sh) 234(4.32)	340(sh)	299(6.47)
$[Ru(bpz)_2(dbpq)]^{2+}$	450(1.48) 230(1.55)	395(1.56)	355(sh)	300(6.36)
$[Ru(dbpq)_2(bpy)]^{2+}$	530(b,sh) 284(8.42)	460(1.15) 256(sh)	388(1.77)	331(sh)
$[Ru(dpp)_2(bpy)]^{2+}$	465(1.46) 250(sh)	428(sh)	285(7.25)	254(3.62)
$[Ru(dmbpy)_2(bpy)]^{2+}$	455(1.46) 286(9.62)	431(sh) 256(sh)	394(sh) 247(2.66)	355(sh) 322(sh)
$[Ru(pyq)_2(bpy)]^{2+}$[b]	495(sh) 274(5.49)	479(1.05) 253(4.31)	460(sh) 247(4.39)	308(4.25) 289(4.48)
$[Ru(dbpq)_3]^{2+}$	496(1.35) 279(10.40)	471(sh)	383(b, sh)	327(b, sh)

[a]sh = shoulder; b = broad. [b]Results in Tables 1–3 for $[Ru(pyq)_2(bpy)]^{2+}$ from refs. 39–41 and this work are included in order to study the behaviour of pyq.

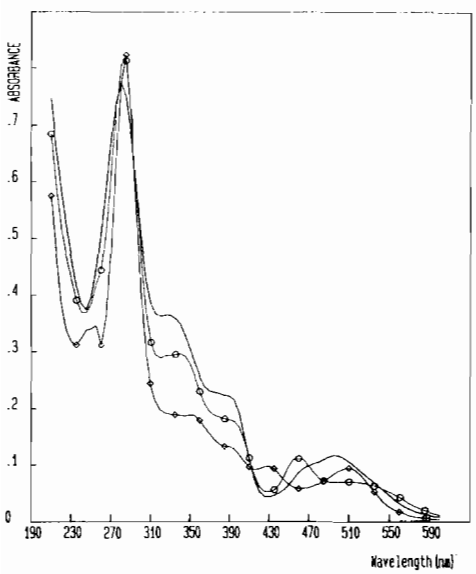

Fig. 1. UV–Vis spectra of $[Ru(dbpq)_3]^{2+}$ (——), $[Ru(dbpq)_2(bpy)^{2+}$ (–○–) and $[Ru(dbpq)(bpy)_2]^{2+}$ (–◇–) in acetonitrile.

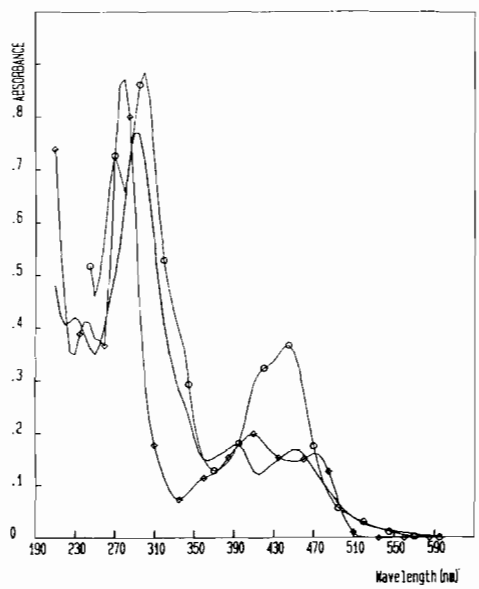

Fig. 2. UV–Vis spectra of $[Ru(bpz)_2(dbpq)]^{2+}$ (——), $[Ru(bpz)_2(bpd)]^{2+}$ (–○–) and $[Ru(bpy)_2(bpd)]^{2+}$ (–◇–) in acetonitrile.

that the mixed ligand complex exhibits bpd peaks at 414, 276 and 234 nm. bpz peaks appear at 340 and 289 nm while the low energy peak at 446 is only slightly red shifted from $[Ru(bpz)_3]^{2+}$, but the closeness of the peaks could indicate a mixed bpd–bpz origin.

The peaks of $[Ru(bpy)_2(bpd)]^{2+}$ [42] at 410 and 360 (shoulder) nm may be assigned to bpd ($d\pi$–π^*) peaks. Other peaks are mixed bpy/bpd peaks, since the spectra for the tris bpy and bpd complexes are close to each other and only the 278 nm peak can be truly related to bpy. The 472 MLCT band is

difficult to assign by comparison to the tris complexes. However, it will be shown later, that, in general, the π^* orbital is lower in the bpd ligand as well as in the tris bpd complex than those of bpy. Thus it is safe to assume that the band in question is due to bpd.

Figure 3 shows peaks at 256, 247, 322(sh) and 255(sh) nm in $[Ru(dmbpy)_2(bpy)]^{2+}$ and these are definitely due to bpy. The 286 nm peak is of mixed origin by comparison to $[Ru(dmbpy)_3]^{2+}$ (459, 450, 362 and 288 nm [33, 39]). Other peaks are more difficult to identify although the low energy MLCT band at 455 nm should be bpy-related since the π^* orbital is generally of lower energy in bpy compared to dmbpy. $[Ru(dpp)_2(bpy)]^{2+}$ exhibits bpy peaks at 285 nm which masks the dpp π–π^* peak at 294 nm [30, 40]. The MLCT peaks at 465 nm are due to dpp. Comparison of results for $[Ru(pyq)_3]^{2+}$ in the literature [43, 44] with those for $[Ru(pyq)_2bpy]^{2+}$ and $[Ru(pyq)(bpy)_2]^{2+}$ [39, 40] shows that a blue shift occurs due to bpy. Our results for $[Ru(pyq)_2bpy]^{2+}$ exhibit the opposite effect (484 nm [44] is shifted to 495 nm in Table 1). We believe our results are correct since they fall in line with cyclic voltammetry and luminescence results. In Fig. 3 the peaks for $[Ru(pyq)_2bpy]^{2+}$ at 460, 289, 253 and 247 nm are related to bpy, while those at 308 and 274 nm could be due to pyq (compared to 313 and 263 nm for $[Ru(pyq)_3]^{2+}$ [43]).

Characteristics of the excited state

Figures 4 and 5 give the room temperature and 77 K luminescence spectra of $[Ru(dbpq)_2(bpy)]^{2+}$

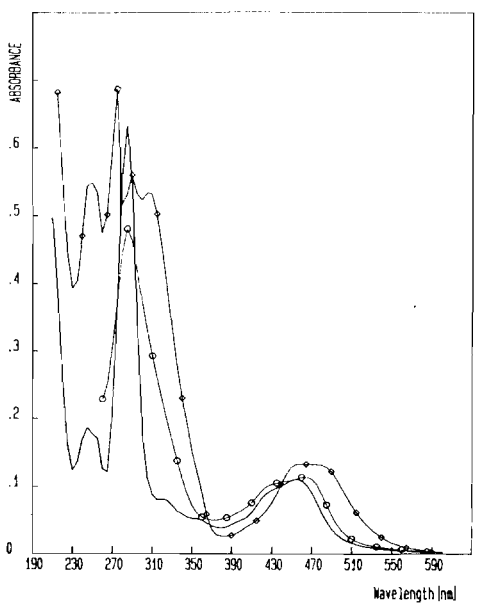

Fig. 3. UV–Vis spectra of $[Ru(dmbpy)_2(bpy)]^{2+}$ (——), $[Ru(dpp)_2(bpy)]^{2+}$ (–○–) and $[Ru(pyq)_2(bpy)]^{2+}$ (–◇–) in acetonitrile.

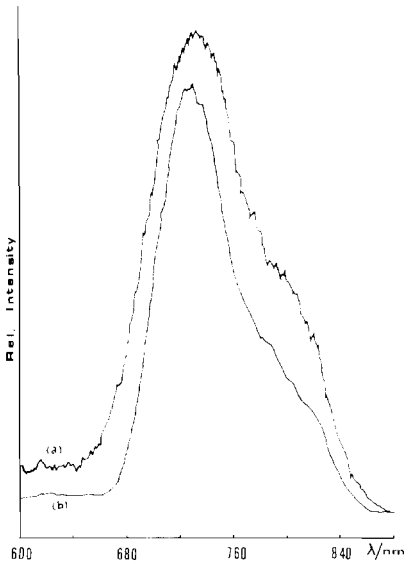

Fig. 4. Room temperature (a) and 77 K (b) luminescence spectra of $[Ru(dbpq)_2(bpy)]^{2+}$ in acetonitrile. $\lambda_{exc} = 476$ nm.

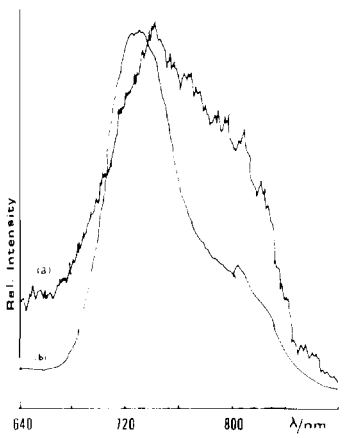

Fig. 5. Room temperature (a) and 77 K (b) luminescence spectra in acetonitrile. $\lambda_{exc} = 476$ nm.

and $[Ru(dbpq)(bpy)_2]^{2+}$, respectively. Table 2 summarizes the results for the ^{3}MLCT states of our complexes. The lifetimes range from 25 to 553 ns. The 77 K spectra often show a blue shift in the maximum, sometimes with a new vibrational band red shifted to the room temperature spectrum. The new bands appear as a result of the freezing of the orientation of dipoles in a way that favours some particular vibrational transitions. The excited state reduction potentials $E^*(3+/2+)$ and $E^*(2+/1+)$ have been calculated from the cyclic voltammetry results in Table 3 and the emission maxima at 77 K. The latter is used as a lower limit to the 0–0 transition energy which is difficult to locate in the

TABLE 2. ^{3}MLCT properties

Complex	λ_{em} (nm)[a]		Lifetime (ns)[a]	$E^*(+3/+2)$	$E^*(+2/+1)$
	Room temperature	77 K			
$[Ru(bpy)_2(bpd)]^{2+}$	700	668, 710(sh)	138	−0.47	0.86
$[Ru(bpy)_2(dbpq)]^{2+}$	740	723, 784(sh)	25	−0.32	0.95
$[Ru(bpz)_2(bpd)]^{2+}$	616	600, 640	553	−0.23	1.31
$[Ru(bpz)_2(dbpq)]^{2+}$	669	654	64	−0.04	1.35
$[Ru(dbpq)_2(bpy)]^{2+}$	730	724, 780(sh)	48	−0.19	1.08
$[Ru(dpp)_2(bpy)]^{2+}$	644	628, 670(sh)	343	−0.48	1.03
$[Ru(dmbpy)_2(bpy)]^{2+}$	628	605, 644	224	−0.85	0.75
$[Ru(pyq)_2(bpy)]^{2+}$	688	676	244	−0.49	0.83
$[Ru(dbpq)_3]^{2+}$	712	698	68	−0.12	1.15
$[Ru(bpy)_3]^{2+}$ [31]	610	580	850[b]	−0.83	0.76

Lifetimes were determined for N_2-degassed solutions with laser excitation at 355 nm. λ_{exc} for steady state measurements was 476 nm. [a]In acetonitrile. [b]in propylene carbonate.

TABLE 3. Reduction and oxidation halfwave potentials[a]

Complex	Reductions (V)	Oxidations (V)	ΔE (V)
$[Ru(bpy)_2(bpd)]^{2+}$	−1.00(80); −1.47(70); −1.72(100)	1.39(80)	2.39
$[Ru(bpy)_2(dbpq)]^{2+}$	−0.77(80); −1.38(160); −1.64(220)	1.39(70)	2.16
$[Ru(bpz)_2(bpd)]^{2+}$	−0.76(70); −0.92(70); −1.25(80)	1.84(80)	2.60
$[Ru(bpz)_2(dbpq)]^{2+}$	−0.64(80); −0.83(60); −1.08(80)	1.95(170)	2.59
$[Ru(dbpq)_2(bpy)]^{2+}$	−0.63(70); −0.87(70); −1.47(80)	1.52(70)	2.15
$[Ru(dpp)_2(bpy)]^{2+}$	−0.94(70); −1.15(70); −1.58(120)	1.49(80)	2.43
$[Ru(dmbpy)_2(bpy)]^{2+}$	−1.30(90); −1.50(90); −1.86(100)	1.20(90)	2.50
$[Ru(pyq)_2(bpy)]^{2+}$	−1.075(90); −1.295(70); −1.695(110)	1.30(80)	2.375
$[Ru(dbpq)_3]^{2+}$	−0.63(60); −0.82(100); −1.09(70)	1.66(70)	2.29

[a]Values in brackets are the difference (in mV) between the anodic and cathodic peaks. Reductions were carried out in DMF and oxidations in acetonitrile. See text for full experimental conditions. ΔE is the difference between the oxidation and the first reduction potentials.

broad spectrum. The calculation assumes minor geometric differences in the ground and excited states and utilizes the equations $E^*(3+/2+) = E(3+/2+) - E_{0-0}$ and $E^*(2+/1+) = E(2+/1+) + E_{0-0}$ [31]. For comparison, we include the results of $[Ru(bpy)_3]^{2+}$ [31]. It is clear from the Table that, except for $[Ru(dmbpy)_2(bpy)]^{2+}$, all the excited states of the complexes are better oxidizing agents than in the case of $[Ru(bpy)_3]^{2+}$. In contrast, they are all weaker reducing agents, except for $[Ru(dmbpy)_2bpy]^{2+}$ which has excited state redox properties almost identical to $[Ru(bpy)_3]^{2+}$.

The shifts that usually occur in the UV–Vis lowest absorption maxima of mixed-ligands complexes relative to the tris complexes are also observed in the emission maxima (both at room temperature (r.t.) and at 77 K). Thus, $[Ru(bpy)_2(bpd)]^{2+}$ (700 nm at r.t.; 668 at 77 K) exhibits a red shift compared to $[Ru(bpd)_3]^{2+}$ (636, 601 nm [32, 33]). Similarly, $[Ru(bpy)_2(dbpq)]^{2+}$ and $[Ru(bpy)(dbpq)_2]^{2+}$ follow this trend compared to $[Ru(dbpq)_3]^{2+}$. This tendency applies to all complexes in which bpy replaces dpp (tris complex: 640, 624 nm [30]) and pyq (tris complex: 658 nm at 77 K [45, 46]). bpz causes a blue shift in $[Ru(bpz)_2(dbpq)]^{2+}$. Similarly, dmbpy red shifts the maxima in $[Ru(dmbpy)_2(bpy)]^{2+}$ compared to $[Ru(bpy)_3]^{2+}$. Except for $[Ru(bpz)_2(dbpq)]^{2+}$ all the low energy absorption maxima of the mixed ligand complexes are red shifted by comparison to the tris complex containing the ligand with the lower π^* orbital (the relative π^* energies are determined from cyclic voltammetry in the following section). The shifts observed can be explained using cyclic voltammetry (see below). However, the similarity between the behaviour of the low energy singlet MLCT absorption maxima and the luminescent triplet MLCT state strongly indicates that the two states originate from the same orbital configuration. The blue shift in the absorption maxima for $[Ru(bpz)_2(dbpq)]^{2+}$ mentioned above could be due to the strong π-acceptor properties of bpz which stabilize the d_π metal orbitals and blue shifts the MLCT band to

dbpq. A direct confirmation of the similar origin of the ^{1}MLCT and ^{3}MLCT states can be obtained from a plot of the energy of the absorption maxima and that of the luminescence spectra versus the difference between the oxidation potential and the first reduction potential of the complex [31, 33, 45–51]. Such potentials yield the relative metal (d_π) and ligand (π^*) energies and therefore the absorption and emission maxima should correlate well with the difference between them. Such expectations are confirmed in Figs. 6 and 7 which include our results as well as those of various tris complexes from the literature. Most striking are the almost identical slopes obtained in both Figures, thus confirming that in the low energy MLCT states, excitation occurs to the π^* orbitals of the ligand with lower π^* energy. If in the mixed complex two molecules of this particular ligand are found, then the question of the localization of the electron on one such molecule or delocalization over both moieties needs further evidence (cyclic voltammetry, ^{3}MLCT transient absorption, excited state resonance raman spectroscopy, etc.).

Cyclic voltammetry results

Table 3 includes the cyclic voltammetry results showing the reduction and oxidation half wave potentials and the difference (ΔE) between the oxidation and first reduction potentials. Figure 8 shows a typical

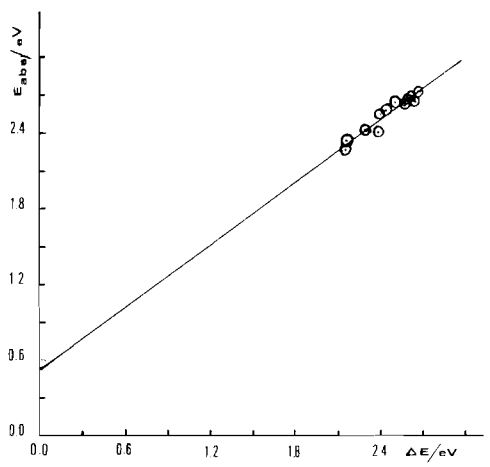

Fig. 6. Energy of the longest λ absorption (at room temperature) (E_{abs}) vs. ΔE (the difference between the oxidation and the first reduction potentials) for the complexes. (Slope = 0.852, intercept = 0.546 eV, and the correlation coefficient = 0.96.) Data is plotted for the following complexes: $[Ru(bpy)_3]^{2+}$, $[Ru(bpz)_3]^{2+}$, $[Ru(bpd)_3]^{2+}$, $[Ru(dbpq)_3]^{2+}$, $[Ru(dpp)_3]^{2+}$, $[Ru(bpy)_2(bpd)]^{2+}$, $[Ru(bpz)_2(bpd)]^{2+}$, $[Ru(bpz)_2(dbpq)]^{2+}$, $[Ru(bpy)_2(dbpq)]^{2+}$, $[Ru(dbpq)_2(bpy)]^{2+}$, $[Ru(dpp)_2(bpy)]^{2+}$, $[Ru(dmbpy)_2(bpy)]^{2+}$, $[Ru(pyq)_2(bpy)]^{2+}$, $[Ru(pyq)_3]^{2+}$, $[Ru(dmbpy)_3]^{2+}$.

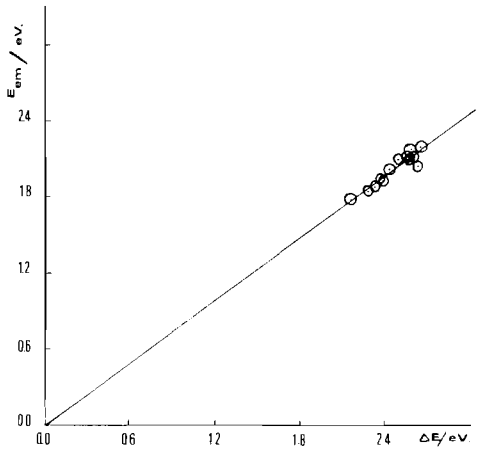

Fig. 7. Energy of the maximum emission (77 K) vs. ΔE (the difference between the oxidation and the first reduction potentials) for the complexes. (Slope = 0.861, intercept = −0.155, and the correlation coefficient = 0.95.) Data is plotted for the same compounds as in Fig. 6.

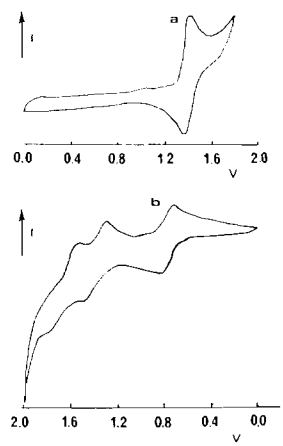

Fig. 8. Cyclic voltammetry of $[Ru(bpy)_2(dbpq)]^{2+}$ over a Pt working electrode against an SSCE reference electrode and a Pt counter electrode. Supporting electrolyte was 0.1 M tetra-n-butylammonium hexafluorophosphate. (a) Oxidation in acetonitrile; (b) reductions in DMF.

voltammogram of $[Ru(bpy)_2(dbpq)]^{2+}$. All our complexes show a single oxidation peak. Three reduction peaks are also observed. Most of the peaks are reversible or quasi-reversible peaks. The oxidation peaks correspond to the removal of an electron from the HOMO metal d-orbital and hence gives an idea about the relative stability of this orbital. By contrast, the three reduction peaks correspond to consecutive placement of an electron in each of the three ligands with the first reduction occurring in the ligand with the lowest energy π^* orbital [15, 30, 31, 33, 43]. Thus the first reduction potential indicates the relative stability of the LUMO π^* orbitals. Similarly, the relative π^* energies in the free ligands can be

determined. Based on results in the literature and the present work this trend is: dmbpy [33] (−2.4 V) > bpy [31] (−2.21) > dpp [30] (−1.90) > bpd [32, 33] (−1.84) > pyq (−1.80) > bpz [31] (−1.76) > dpq [15] (−1.56) > dbpq (−1.55) (the more negative the potential the higher the π^* energy). Upon complexation, the π^* orbitals are stabilized by about 1 V in the tris complexes and this results in a linear relationship between the first reduction potentials of the complexes and those of the ligands [15, 43]. The known trend for the complexes first reduction is only slightly different from that of the ligand: $[Ru(dmbpy)_3]^{2+}$ (−1.46 [41] or −1.34 [52]) > $[Ru(bpy)_3]^{2+}$ (−1.31 [31]) > $[Ru(pyq)_3]^{2+}$ (−1.05 [41]) > $[Ru(bpd)_3]^{2+}$ (−1.00 [33]) > $[Ru(dpp)_3]^{2+}$ (−0.95 [40]) > $[Ru(bpz)_3]^{2+}$ (−0.68 [31]) > $[Ru(dbpq)_3]^{2+}$ (−0.63) > $[Ru(dpq)_3]^{2+}$ (−0.60) [15]. Comparison of these values with the mixed-ligand complexes in Table 3 shows that the first reduction potentials almost follow this trend (provided that comparison is made for the tris complex that has the lower energy π^* state in the mixed ligand complex). The following trend for the mixed complexes also indicates (with a star) the ligand into which the first reduction occurs:

$[Ru(dmbpy)_2(bpy)^*]^{2+} > [Ru(pyq)^*_2(bpy)]^{2+} >$

$[Ru(bpy)_2(bpd)^*]^{2+} > [Ru(dpp)^*_2(bpy)]^{2+} >$

$[Ru(bpy)_2(dbpq)^*]^{2+} > [Ru(bpz)^*_2(bpd)]^{2+} >$

$[Ru(bpz)_2(dbpq)^*]^{2+} > [Ru(dbpq)^*_2(bpy)]^{2+}$

The relative metal orbital stability of the complexes is indicated by the oxidation potentials. The higher this potential is, the more stable is the metal orbital [31]. Thus in the tris complexes the relative energy of the metal d-orbitals (which are available for π backdonation to the ligands) follows the trend:

$[Ru(bpz)_3]^{2+}(1.98) < [Ru(dpq)_3]^{2+}(1.70) <$

$[Ru(dpp)_3]^{2+}(1.68) < [Ru(dbpq)_3]^{2+}(1.66) <$

$[Ru(bpd)_3]^{2+}(1.58) < [Ru(pyq)_3]^{2+}(1.33) <$

$[Ru(bpy)_3]^{2+}(1.27) < [Ru(dmbpy)_3]^{2+}$

(1.10 or 1.17) (the values are obtained from the same references as for the first reduction potentials).

σ and π properties of the ligands

The relative stability of the metal orbitals and the π^* orbitals depend on the σ-donor and π-acceptor properties of the ligands [30–34]. Strong σ donation increases the electron density on the metal, thus destabilizing the metal HOMO orbitals, and to a lesser extent the π^* orbitals of the ligand [34, 48, 53]. On the other hand stronger π bonding stabilizes the metal orbitals and destabilizes the π^* orbitals [34, 48, 53]. It is thus possible to analyze the data for the first reduction potentials and the oxidation potentials in order to gauge the donor and acceptor properties of the ligands. The best approach [30, 31] is to compare the tris complexes of two ligands and develop a feeling for which ligand is a better σ donor and which is the better π acceptor. This conclusion can then be confirmed by analyzing the redox potentials of the mixed-ligand complexes. Further confirmation is obtained by studying the shifts in the MLCT spectra (lowest energy UV–Vis peak and luminescence) of the mixed-ligand and the tris complexes. Such an approach has been utilized to compare bpz, bpy and bpm (2,2′-bipyrimidine [31] with each other. Similarly, other ligands [30] have been compared with bpy and bpz. The σ-donor ability of the following pairs is well established: dpq > bpz; bpy > dpq [30] and bpy > bpz [31]. The π-acceptor trend is exactly the opposite. In the following discussion, only a number of examples will be used to illustrate the arguments since an exhaustive discussion of all the pair-combinations will be too long.

Considering bpy and dbpq, the ligand reduction potentials (−2.21 and −1.55 V, respectively) indicate a lower π^* orbital in dbpq. Upon tris-complexation the π^* orbitals are stabilized to −1.31 and −0.63 V, respectively. The oxidation potentials indicate that the metal orbital in $[Ru(dbpq)_3]^{2+}$ (1.66 V) is more stable than in $[Ru(bpy)_3]^{2+}$ (1.27). This seems to indicate larger destabilization by bpy due to its stronger σ donation. The π^* orbitals are stabilized by about the same amount (0.90 and 0.92 V). The difference in metal orbital stability is 0.39 V but the difference in ΔE is only 0.29 V (2.58 V for $[Ru(bpy)_3]^{2+}$ and 2.29 V for the dbpq complex). This seems to favour a better π-acceptor ability for dbpq. To confirm this the series $[Ru(dbpq)_3]^{2+}$, $[Ru(dbpq)_2(bpy)]^{2+}$ and $[Ru(bpy)_2(dbpq)]^{2+}$ show a respective destabilization of the metal orbital (1.66, 1.52, 1.39 V) due to the better σ donation of bpy and a trend in ΔE of (2.29, 2.15 and 2.16 V). This ΔE trend predicts red shifts in the MLCT absorption and luminescence peaks at room temperature and 77 K (496, 530, 510 nm and 712, 730, 740 nm and 698, 724, 723 nm, respectively). Thus in the mixed ligand complexes the strong σ donation of bpy destabilizes the metal orbital reducing the energy gap. The increased electron density on the metal should enhance π backdonation to dbpq thus lowering the metal orbital and raising the dbpq π^* orbital. Since π^* destabilization is less than the metal orbital destabilization, it is obvious dbpq is only slightly better as a π acceptor.

For bpz and dbpq, the reduction potentials in the ligand and the tris complexes are lower for dbpq which thus has a lower π^* orbital. The metal orbital is more stable in $[Ru(bpz)_3]^{2+}$ (1.98 versus 1.66 V) indicating better σ donation for dbpq, but the closeness of the π^* energies (−0.68 versus −0.63 V) and the larger energy gap, ΔE (2.66 V for $[Ru(bpz)_3]^{2+}$ and 2.29 V for $[Ru(dbpq)_3]^{2+}$), strongly favours bpz as the superior π acceptor. Substitution of two bpz molecules in $[Ru(dbpq)_3]^{2+}$ confirms the weaker σ-donor ability of bpz by stabilization of the metal orbital. The π donation to dbpq in the mixed complex is quite limited due to the lowered electron density on the metal and the stronger π-acceptor power of bpz. This results in a higher ΔE (2.59 V) in the mixed complex with the prediction of a blue shift in the MLCT peaks. The low energy absorption peak at 496 nm in $[Ru(dbpq)_3]^{2+}$ is certainly blue shifted (450 nm) in $[Ru(bpz)_2(dbpq)]^{2+}$. Similarly, the room temperature and 77 K emission maxima are blue shifted.

Comparison of $[Ru(bpz)_3]^{2+}$ and $[Ru(bpd)_3]^{2+}$ shows stabilization of the ligand π^* orbital from −1.76 to −0.68 V in the first case and from −1.84 to −1.00 V in the second. The bpz π^* orbital is of lower energy and the stabilization due to bpz is higher upon complexation. The metal orbital in $[Ru(bpz)_3]^{2+}$ is lower in energy (1.98 V versus 1.84 V) thus indicating better σ donation in bpd, while the higher ΔE (in $Ru(bpz)_3^{2+}$ = 2.66 versus 2.58 V), despite the better stabilization of the π^* orbital for bpz, strongly indicates better π acceptance in bpz. Substitution of bpd in $[Ru(bpz)_3]^{2+}$ destabilizes both the metal and the π^* orbitals (1.98 to 1.84 V and −0.68 to −0.76 V). Thus the stronger σ bonding of bpd destabilizes the metal orbital. The resulting increase in electron density on the metal enhances even more the π backdonation to bpz thus raising its π^* orbital (−0.76) compared to the tris complex (−0.68). This results on the whole in a lower ΔE (2.60 versus 2.66 V) and the prediction of a red shift in the MLCT spectra. This is true for the absorption spectra (446 from 440 nm), the room temperature emission (616 from 610 nm) and the 77 K emission (600 from 573 nm).

As a last example we consider bpy and pyq. In the ligands and tris complexes pyq has the lower π^* orbital (−1.80 and −1.09 V [41] for pyq and −2.21 and −1.31 V for bpy). Furthermore, the oxidation potential in $[Ru(pyq)_3]^{2+}$ is 1.333 [5] versus 1.27 V in $[Ru(bpy)_3]^{2+}$, thus indicating less stable metal orbitals in the latter and hence bpy exhibits slightly better σ-donor properties. This is borne out by the results for $[Ru(pyq)_2bpy]^{2+}$ in which the metal orbital is destabilized (1.333 to 1.30 V [44]) by the replacement of pyq by one bpy. The introduction of another bpy further destabilizes the σ orbital (1.27 V). On the other hand, a bpy molecule does not alter appreciably the π^* level (−1.085 to −1.075 V [44] while two bpy molecules cause a slight π^* destabilization (−1.085 to −1.135 V [44]). This indicates a slightly better π-acceptor property of bpy. The ΔE values in $[Ru(pyq)_2(bpy)]^{2+}$ (2.375 versus 2.418 V) in $[Ru(pyq)_3]^{2+}$ predict a red shift in the low energy MLCT absorption peak (495 versus 484 nm [44]) and the luminescence maxima (676 versus 658 nm) at room temperature and (688 versus 687 nm [44]) at 77 K.

Based on our analysis of the pairwise comparison of the ligands, we arrive at the conclusion that σ donation follows the decreasing trend: dmbpy > bpy > bpd > dpp > dbpq ≥ dpq > bpz while the π acceptor ability follows: bpz > dpq > dbpq ≥ dpp > bpd > bpy > dmbpy.

It is interesting to note that the observed trend for bpy and dmbpy, where dmbpy exhibits slightly better σ donation and slightly weaker π-acceptor properties exhibited in the red shift of the bpy ^{3}MLCT luminescence and the ^{1}MLCT lowest absorption peak is not surprising due to the electron releasing property of the methyl groups.

A number of the pairwise comparisons had to rely on the tris complexes alone, since no mixed-ligand complexes are known for such pairs (e.g. dpp and dpq). We attempted to confirm our conclusions by comparing the effect of these pairs on the second reduction potentials into the π^* orbitals of bpy in complexes of the type $[Ru(bpy)_2dpp]^{2+}$ and $[Ru(bpy)_2dbpq]^{2+}$. Attempts to explain the trends in the second reduction potentials by means of the σ and π abilities of the pairs gave inconsistent predictions. However, we noted that a correlation exists between the second and first reduction potentials in complexes of the type $[Ru(bpy)_2L]^{2+}$. Using values in the literature along with those in this work, a linear regression programme was used to analyze results for complexes of the type $[Ru(bpy)_2L]^{2+}$ and $[Ru(bpz)_2L]^{2+}$. Unfortunately, while a good correlation coefficient for our own complexes was obtained, only values of 0.81 and 0.84, respectively were obtained when literature values were included. Nevertheless, a qualitative trend cannot be ignored and the poor correlation may be due to the closeness of the values of different complexes (often lying within the experimental error of the cyclic voltammetry experiment). The qualitative trend could be explained as follows: The introduction of an electron into the π^* of L repels the π^* orbitals of bpy (or bpz) where the second electron is to be placed. The higher the π^* orbital of L (i.e. the more

negative is the first reduction potential), the higher the π^* orbital of bpy or bpz would be repelled and the more negative the second reduction potential is. Alternatively, the additional negative charge of the ligand L enhances its σ donation to the metal atom and reduces the π backdonation to L. The increased negative charge on the metal atom enhances π backdonation to the bpy (or bpz) π^* orbitals thus raising its energy. The higher the π^* orbital of L is, the stronger is the need for π donation to the metal to compensate for the destabilization, and the poorer the π-acceptor power of L becomes. This would raise the π^* orbital of bpy (or bpz) even more. Hence, the decrease of the second reduction potential with more negative first reduction potentials can be qualitatively explained.

Conclusions

UV–Vis absorption and luminescence spectra along with cyclic voltammetry provide powerful tools for the prediction of the redox behaviour of ^{3}MLCT states of Ru(II)–diimine complexes. Furthermore, the σ and π behaviour of the ligands can be easily predicted from such techniques.

Acknowledgements

T.S.A. gratefully acknowledges the financial support of Yarmouk University, the Ministry of Planning in Jordan and the Kuwait Development Fund. This work is part of the M.Sc Thesis of A.M.S.

References

1 (a) K. Kalyanasundaram, *Coord. Chem. Rev., 46* (1982) 159; (b) A. Juris, V. Balzani, F. Barigelletti, S. Campagna, P. Belser and A. Von Zelewsky, *Coord. Chem. Rev., 84* (1988) 85.
2 M. K. DeArmond and C. M. Carlin, *Coord. Chem. Rev., 36* (1981) 325.
3 N. Sutin and C. Creutz, *Pure Appl. Chem., 52* (1980) 2717.
4 D. G. Whitten, *Acc. Chem. Res., 13* (1980) 83.
5 T. J. Meyer, *Pure Appl. Chem., 58* (1986) 1193.
6 K. Kalyanasundaram, J. Kini and M. Gratzel, *Helv. Chim. Acta, 61* (1978) 6270.
7 R. J. Crutchley and A. B. P. Lever, *J. Am. Chem. Soc., 102* (1980) 7128.
8 J. K. Nagle, R. C. Young and T. J. Meyer, *Inorg. Chem., 16* (1977) 3366.
9 D. R. Prasad and M. Z. Hoffman, *J. Am. Chem. Soc., 108* (1986) 2568.
10 D. R. Prasad, D. Hessler, M. Z. Hoffman and N. Serpone, *Chem. Phys. Lett., 121* (1985) 61.
11 D. R. Prasad, K. Mandal and M. Z. Hoffman, *Coord. Chem. Rev., 64* (1985) 175.
12 R. V. Bensasson, C. Salet and V. Balzani, *J. Am. Chem. Soc., 98* (1976) 3722.
13 T. S. Akasheh, P. C. Beaumont, B. J. Parsons and G. O. Phillips, *J. Phys. Chem., 90* (1986) 5651.
14 K. R. Barqawi, T. S. Akasheh, P. C. Beaumont, B. J. Parsons and G. O. Phillips, *J. Phys. Chem., 92* (1988) 291.
15 D. P. Rillema, D. C. Taghdiri, D. S. Jones, C. D. Keller, L. A. Worl, T. J. Meyer and H. A. Levy, *Inorg. Chem., 26* (1987) 578.
16 F. Barigelletti, A. Juris, V. Balzani, P. Belser and A. Von Zelewski, *J. Phys. Chem., 91* (1987) 1095.
17 F. Barigelletti, P. Belser, A. Von Zelewski, A. Juris and V. Balzani, *J. Phys. Chem., 89* (1985) 3680.
18 W. M. Wacholtz, R. A. Auerbach and R. H. Schmehl, *Inorg. Chem., 25* (1986) 227.
19 G. D. Van Houten and R. J. Watts, *Inorg. Chem., 17* (1978) 3381.
20 B. Durham, J. V. Caspar, J. K. Nagle and T. J. Meyer, *J. Am. Chem. Soc., 104* (1982) 4803.
21 J. V. Caspar and T. J. Meyer, *Inorg. Chem., 22* (1983) 2444.
22 J. V. Caspar and T. J. Meyer, *J. Am. Chem. Soc., 105* (1983) 5583.
23 G. H. Allen, R. P. White, D. P. Rillema and T. J. Meyer, *J. Am. Chem. Soc., 106* (1984) 2613.
24 L. H. Henderson, F. Fronczek and W. R. Cherry, *J. Am. Chem. Soc., 106* (1984) 5876.
25 W. R. Cherry and L. H. Henderson, *Inorg. Chem., 23* (1984) 983.
26 D. V. Pinnick and B. Durham, *Inorg. Chem., 23* (1984) 3841.
27 A. Juris, F. Barigelletti, V. Balzani, P. Belser and A. Von Zelewsky, *Inorg. Chem., 24* (1985) 202.
28 W. M. Wacholtz, R. S. Auerbach, R. H. Schmehl, M. Ollino and W. R. Cherry, *Inorg. Chem., 24* (1985) 1758.
29 K. R. Barqawi, A. Llobet and T. J. Meyer, *J. Am. Chem. Soc., 110* (1988) 7751.
30 T. S. Akasheh and Z. M. El-Ahmad, *Chem. Phys. Lett., 152* (1988) 414.
31 D. P. Rillema, G. Allen, T. J. Meyer and D. Conrad, *Inorg. Chem., 22* (1983) 1617.
32 N. Kitamura, Y. Kawanishi and S. Tazuke, *Chem. Phys. Lett., 97* (1983) 103.
33 Y. Kawanishi, N. Kitamura, Y. Kim and S. Tazuke, *Sci. Papers Inst. Phys. Chem. Res., 78* (1984) 212.
34 R. J. Crutchley and A. B. P. Lever, *Inorg. Chem., 21* (1982) 2276.
35 D. P. Rillema, R. W. Callahan and K. B. Mack, *Inorg. Chem., 21* (1982) 2589.
36 R. W. Callahan, G. M. Brown and T. J. Meyer, *Inorg. Chem., 14* (1975) 1443.
37 R. A. Krause and K. Krause, *Inorg. Chem., 21* (1982) 1714.
38 I. Jibril, T. S. Akasheh and A. M. Shraim, *Polyhedron, 8* (1989) 2615.
39 A. P. Mabrouk and M. Wrighton, *Inorg. Chem., 25* (1986) 527.
40 K. J. Brewer, W. R. Jr. Murphy, S. R. Spurlin and J. D. Peterson, *Inorg. Chem., 25* (1986) 889.

41 W. F. Wacholtz, R. A. Auerbach and R. H. Schmehl, *Inorg. Chem., 26* (1987) 2992.
42 S. D. Ernst and W. Kaim, *Inorg. Chem., 28* (1989) 1520.
43 C. D. Tait, D. B. MacQueen, R. J. Donohoe, M. K. DeArmond, K. W. Hanck and D. W. Wertz, *J. Phys. Chem., 90* (1986) 1766.
44 Y. Ohsawa, K. W. Hanck and M. K. DeArmond, *J. Electroanal. Chem., 175* (1984) 229.
45 D. M. Klassen, *Chem. Phys. Lett., 93* (1982) 383.
46 D. M. Klassen, *Inorg. Chem., 15* (1976) 3166.
47 K. J. Moore and J. D. Peterson, *Polyhedron, 2* (1983) 279.
48 A. B. P. Lever, S. Licoccia, P. C. Minor, B. S. Ramaswamy, S. R. Pickens and K. Magnell, *J. Am. Chem. Soc., 103* (1981) 6800.
49 J. C. Curtis and T. J. Meyer, *Inorg. Chem., 21* (1982) 1562.
50 B. P. Sullivan, J. A. Baumann, T. J. Meyer, D. J. Salmon, H. Lehmann and A. Ludi, *J. Am. Chem. Soc., 99* (1977) 7368.
51 J. V. Caspar and T. J. Meyer, *Inorg. Chem., 22* (1983) 2448.
52 E. M. David, K. W. Hanck and M. K. DeArmond, *J. Am. Chem. Soc., 105* (1983) 3033.
53 R. W. Balk, R. J. Crutchley and A. B. P. Lever, *Inorg. Chim. Acta, L49* (1981) 64.